

Spectral Analysis of Storm Waves Using the Hilbert-Huang Transform.

Joaquín Ortega
CIMAT, A.C.
Guanajuato, Gto., Mexico

George H. Smith
Exeter University
Cornwall Campus, U.K.

ABSTRACT

We use the Hilbert-Huang Transform (HHT) for the spectral analysis of waves during a storm in the North Sea that took place in 1999. We look at the contribution of the different Intrinsic Mode Functions (IMF) obtained by the Empirical Mode Decomposition algorithm and also compare the Hilbert Marginal Spectra and the classical Fourier spectra for the data set and for the corresponding IMFs.

KEY WORDS: Hilbert-Huang Transform; Empirical Mode Decomposition; Intrinsic Mode Function; Spectral Analysis.

INTRODUCTION

The Hilbert-Huang Transform (HHT) was proposed by Huang et al. (1998, 1999, 2003), as an adequate method for the spectral analysis of non-stationary, nonlinear processes. Since then it has been used by several authors for the analysis of sea waves under different conditions (Schlumann, 2000, Veltcheva and Guedes Soares, 2004, Veltcheva, 2005, among others).

In this work we study a storm in the North Sea using the HHT. The wave data was decomposed into Intrinsic Mode Functions and their characteristics are studied and compared to those of the original record. We consider both the Hilbert and Fourier Spectra for comparison.

HHT

We give a brief description of the Hilbert Huang Transform. A detailed presentation can be found in the original articles of Huang et al. (1998, 1999) as well as in Huang (2005a, b).

The Hilbert Huang Transform is based on an empirical algorithm called the Empirical Mode Decomposition (EMD), used to decompose a time series into individual characteristic oscillations known as the intrinsic mode functions (IMF). This technique is based on the assumption that any signal consists of different modes of oscillation based on different time scales, so that each IMF represents one of these embedded oscillatory modes. Each IMF has to satisfy two criteria: 1) The number of local extreme points and of zero-crossings must either be equal or differ at most by one, 2) At any instant, the mean of the envelope defined by the local maxima and the envelope corresponding to the

local minima must be zero. These two conditions are required to avoid inconsistencies in the definition of the instantaneous frequency.

Once the signal is decomposed, the Hilbert Transform is applied to each IMF. The Hilbert transform $y(t)$ of a function $x(t)$ is defined as $(1/\pi)$ times the convolution of f with the function $1/t$. Then, if $z(t)$ is the analytical signal associated to $x(t)$, we have for all t

$$z(t) = x(t) + iy(t) = A(t) \exp(i\theta(t)) \quad (3)$$

with $A(t) = (x^2(t) + y^2(t))^{1/2}$ and $\theta(t) = \arctan(y(t)/x(t))$.

The instantaneous frequency is defined now as the derivative of the phase function of the analytical signal $z(t)$:

$$\omega(t) = \frac{d\theta(t)}{dt} \quad (2)$$

Once the signal has been decomposed into IMFs and the Hilbert transform for each has been obtained, the signal $x(t)$ can be represented as

$$x(t) = \sum_{j=1}^n A_j(t) \exp\left(i \int \omega_j(t) dt\right) \quad (3)$$

which is a generalized form of the Fourier expansion for $x(t)$ in which both amplitude and frequency are functions of time.

The time-frequency distribution of the amplitude or the amplitude squared is defined as the Hilbert amplitude spectrum or the Hilbert energy spectrum, respectively. In this work we use the Hilbert energy spectrum.

DATA

Data was recorded from the North Alwyn platform situated in the northern North Sea, about 100 miles east of the Shetland Islands (60°48.5' North and 1°44.17' East) in a water depth of approximately 130 metres. There are three Thorn EMI Infra-red wave height meters mounted on the platform and their heights are between 25 and 35 metres above the water. The data are recorded continuously and simultaneously at 5Hz and then divided into 20 minute records for which the summary statistics of H_s , T_p and the spectral moments are calculated. For data with $H_s > 3m$ all the surface elevation records are kept. The data was transmitted to Heriot-Watt University on a daily basis, creating the largest, continuously recorded set of Metocean data

on the UK continental shelf. Further details are available in Wolfram et al (1994). Only data from the North East altimeter are used here.

One set of data was examined. It consists of a series of records of 20 minutes duration, sampled by the altimeter at a rate of 5 Hz., and occurred between midnight on December 23rd and 9.00 a.m. on December 26th 1999 and consisted of 244, 20 minute, records. This data starts at a high level with a significant wave height of about 6.5 to 7 m and then drops away to about 3.5 m before increasing back up to around 7 m for around 20 hours. It then reduces again, before increasing to about 6.5 m, dropping to about 5 and then increasing again to around 5.5m before finally dropping to less than 3.5m at the end of the dataset. As such this data includes two relative large increases in H_s and a section in which two peaks occur within relatively short time period.

Since there were some short intervals missing in the data, we divided it into five sets that cover the storm. In Table 1 we give a list of the five sets along with some basic characteristics of the wave records: Significant wave height H_s , mean wave period T_{m01} , spectral peak period T_p and spectral bandwidth parameter ν . Figure 1 shows the evolution of significant wave height and peak period during the storm.

Table 1. Basic characteristics of the five intervals of data.

	Duration	H_s	T_{m01}	T_p	ν	# IMFs
Int. 1	8h. 40m.	5.34	9.31	11.87	0.509	17
Int. 2	6h.	3.72	8.48	11.22	0.514	15
Int. 3	18h.	5.07	8.25	10.50	0.510	19
Int. 4	24h.	5.87	8.99	11.70	0.492	21
Int. 5	24h.	5.10	8.75	11.70	0.506	20

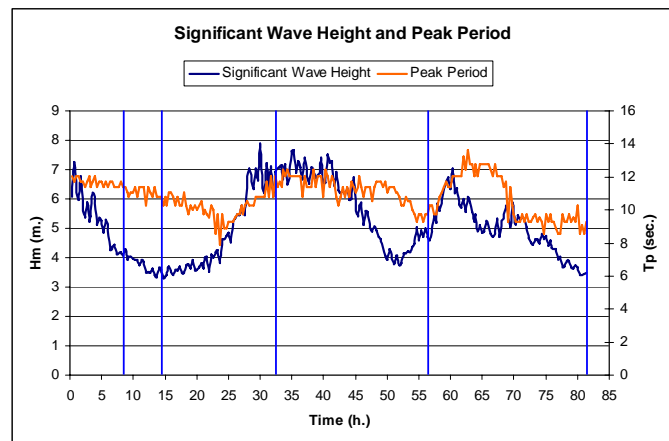


Figure 1. Evolution of significant wave height and peak period.

RESULTS

The five wave records were decomposed into Intrinsic Mode Functions (IMFs) using the Empirical Mode Decomposition process. The software used was HHT-DPS, developed by Nasa. After a number of trials with different sets the sifting criteria was set at 5 siftings and the option Endpoint Prediction for the splines was set to Mean Prediction, which seemed to give the best results in our case.

The number of IMFs obtained varied with each interval and seems to increase with its length, as can be seen in table 1. This is probably due to the fact that longer intervals allow for the detection of lower frequencies in the data.

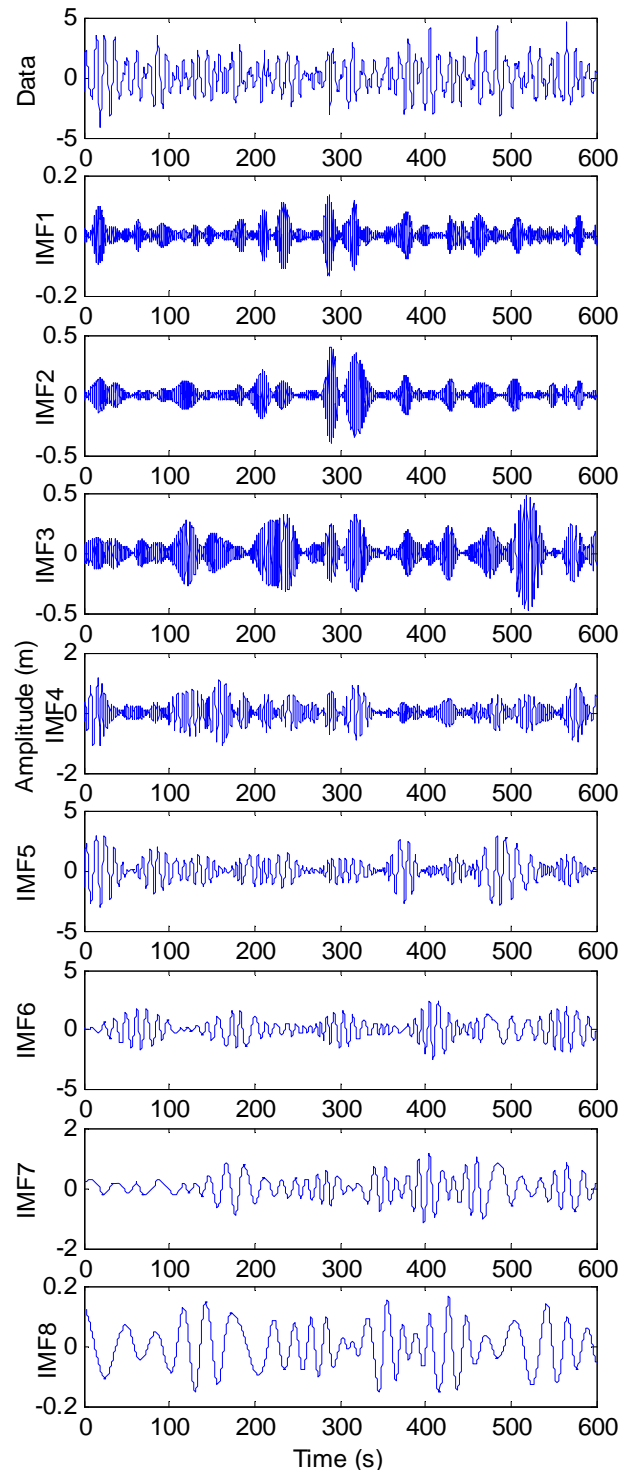


Fig 2 Original data and IMFs 1-8 for Interval 1.

the original data and for each of the 17 IMFs obtained for the first interval.

As is usual for this decomposition, different IMFs correspond to different frequencies, being higher for the first IMF and decreasing thereof. This can readily be seen from Figure 4 which shows the boxplots for the frequency distribution of each of the 17 IMFs corresponding to the first interval. Results for the other time intervals were similar.

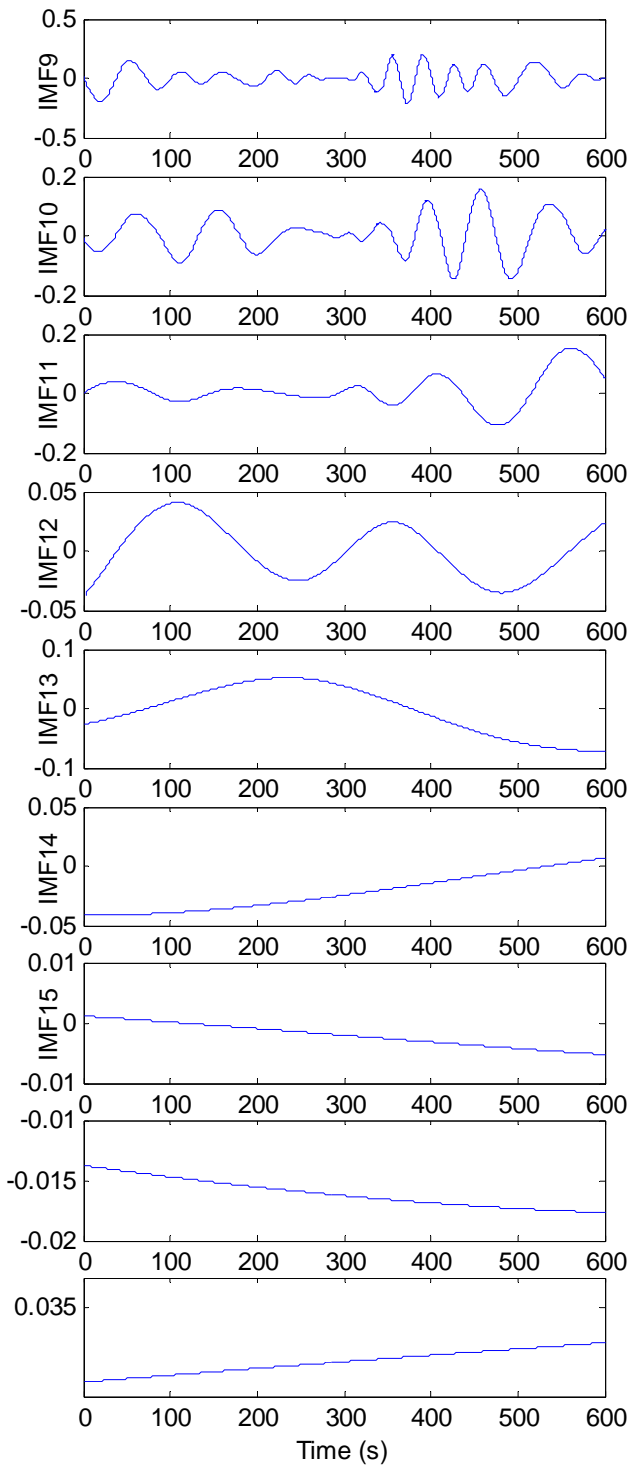


Fig 3 IMFs 9-17 for Interval 1.

Figures 2 and 3 show 10 minutes (at the beginning of the third hour) for

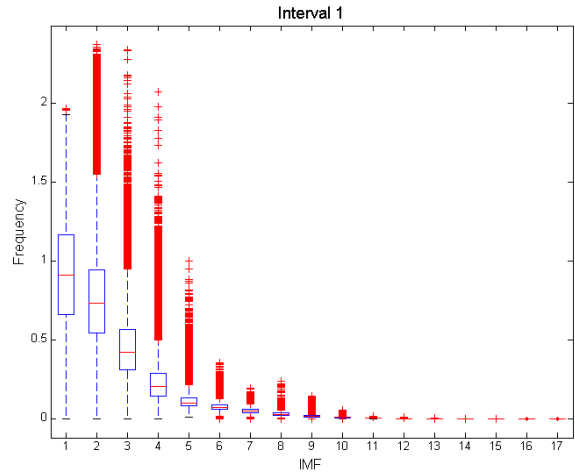


Fig. 4 Boxplot of frequencies for the different IMFs.

Table 2. Variance for each interval

	Int. 1	Int. 2	Int. 3	Int. 4	Int. 5
Variance	1.784	0.864	1.606	2.151	1.626
Sum of Var.	1.821	0.882	1.589	2.102	1.593
% difference	2.05	2.09	1.61	2.27	2.06

Table 3. Contribution of each IMF to the total variance for Interval 1.

	Variance	% of total	Cumulative %
IMF5	0.93735	51.488	51.488
IMF6	0.42806	23.513	75.001
IMF4	0.31390	17.242	92.243
IMF7	0.08808	4.838	97.081
IMF8	0.01615	0.887	97.968
IMF3	0.01572	0.863	98.831
IMF9	0.00679	0.373	99.204
IMF10	0.00376	0.207	99.411
IMF2	0.00367	0.202	99.613
IMF11	0.00271	0.149	99.761
IMF12	0.00183	0.100	99.862
IMF13	0.00103	0.057	99.919
IMF1	0.00077	0.042	99.961
IMF14	0.00034	0.019	99.980
IMF15	0.00016	0.009	99.988
IMF16	0.00013	0.007	99.995
IMF17	0.00008	0.005	100.000
Sum	1.8205	100.000	

The contribution of each IMF to the total energy as measured by the variance (or equivalently, by the zero order spectral moment m_0) is also different. We calculated the variance for the original data and for each IMF, and then obtained the sum of the variances for all IMFs. If the IMFs were orthogonal, these two quantities should be the same, so the difference can be used as a measure of orthogonality. Table 2 gives this comparison for the 5 intervals. As can be seen in all cases the difference was small.

Table 3 gives the contribution to the sum of the variances of each IMF for interval 1, both in absolute terms, percentage of total and the cumulative percentage contribution. It can be seen that the biggest contribution comes from IMF5, with over 51% of the total energy, and that the four most energetic IMFs (5, 4, 6 and 7) account for over 97% of the total energy. Figure 5 shows the boxplots for the amplitudes of each IMF, where the same relationship shows up.

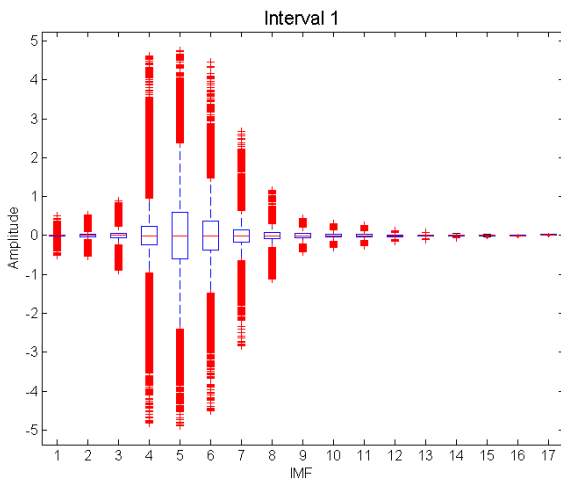


Fig. 5 Boxplot of amplitudes for the different IMFs.

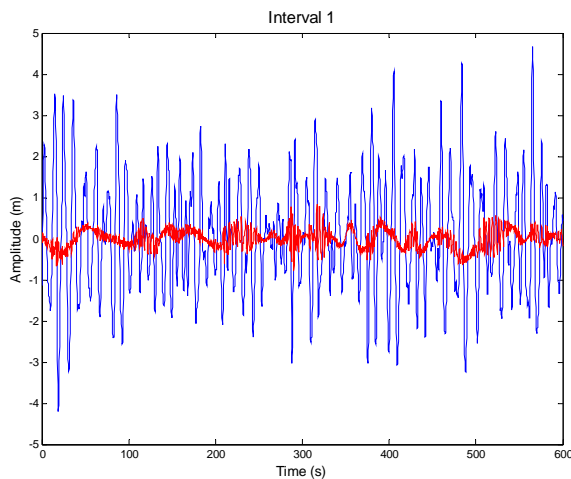


Fig 6 Wave data and remainder after subtracting the sum of IMFs 4, 5, 6 and 7.

Figure 6 shows the same period of time as figures 2 and 3 and compares the original data set and the result of subtracting the sum of the four most energetic IMFs (4-7). As can be seen, the sum has captured most of the large-scale variation in the original signal, but

there is still a lot of information in the remainder.

Similar results were obtained for the other intervals. They are shown in Table 4 in terms of the cumulative percentage contribution of the six most energetic IMFs and in Figure 7 for the 15 first IMFs. For intervals 1 and 2, the four most energetic IMFs account for over 96% of the total variance. For intervals 3 and 5, five IMFs are required to go over 95% and for interval 4, which seems to have the energy more evenly distributed among IMFs, seven are needed to go over 95%.

Table 4. Contribution of the six main IMFs to the total variance for all intervals.

Int. 1	IMF	5	6	4	7	8	3
	% Var.	51.49	75.00	92.24	97.08	97.97	98.83
Int. 2	IMF	4	5	3	6	2	7
	% Var.	59.97	82.48	91.97	96.48	98.13	99.05
Int. 3	IMF	6	7	5	8	4	9
	% Var.	35.28	65.92	80.64	91.88	95.35	97.66
Int. 4	IMF	8	7	9	6	10	5
	% Var.	38.81	55.55	70.16	80.46	90.11	93.93
Int. 5	IMF	7	8	6	9	5	10
	% Var.	41.08	61.46	81.28	91.13	95.36	97.17

This is in contrast to what was reported by Veltcheva and Guedes Soares (2004) for various sea conditions off the Portugal coast and Veltcheva (2005) for various sea conditions off the coast of Japan, where the first three IMFs are the most energetic ones. For example, in the first case, for two of the data sets they analyze in detail, IMF2 is the most energetic followed by IMF3, and for the other data set IMF1 is first followed by IMF2. It should be pointed out, however, that the sets of data for which these authors give a detailed analysis have a much lower significant wave height than the sets we are considering.

It is possible that more complex sea states, such as those that occur during a storm, require more IMFs to decompose them and hence the energy is distributed differently. Thus the main part of the energy is not carried by the very high frequency components but by intermediate ones. In calmer sea states these very high frequency components probably are not present, or if they are, they are less frequent and can be decomposed along with other frequencies in a single IMF.

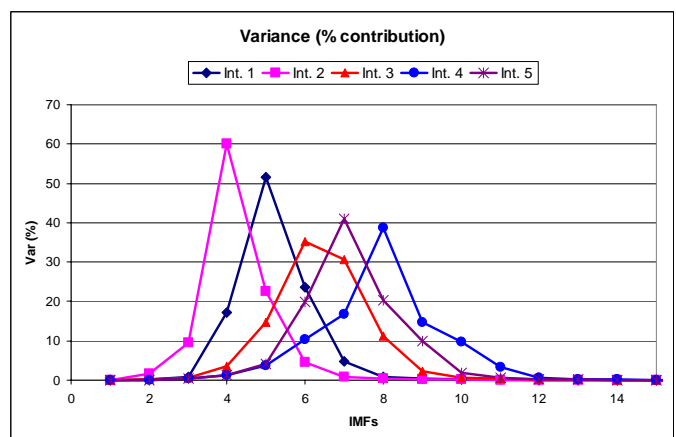


Fig. 7 Contribution of each IMF to the total variance for all time intervals.

Spectral Analysis.

We analyzed both the Fourier spectra and the Hilbert Spectra for the five time intervals but we only present the results corresponding to the first one. Figure 8 gives the Hilbert spectrum with no regularization, as produced by HHT-DPS, where the energy level is given in a color scale. From this graph it is possible to see a detailed record of the variation in frequency and energy with time. For example, one can see that most of the energy is concentrated in a band around a frequency of 0.1 Hz and also that the amount of energy decreases toward the end of the period, which is consistent with the significant wave height evolution (see figure 1). Although there are high frequency components present in the spectrum, most of the energy is in the low frequencies, represented by IMFs 4, 5, 6 and 7.

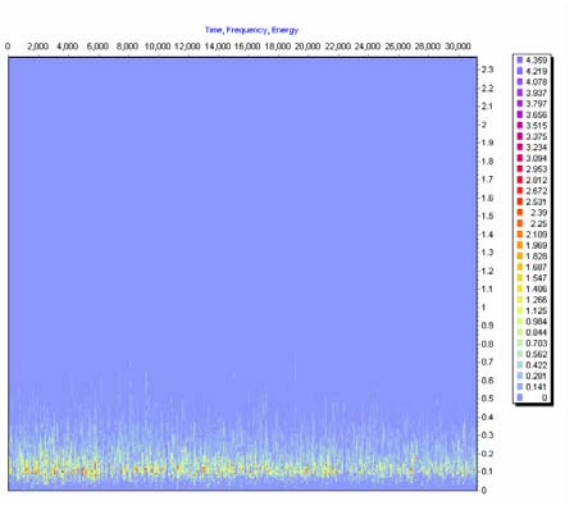


Fig. 8 Hilbert Spectrum for interval 1.

We also considered the Fourier spectra for the original data and for each IMF. They are shown in figure 9. It can be seen from this graph, as was pointed out before, that as the IMF number increases the corresponding frequency range and peak frequency decreases.

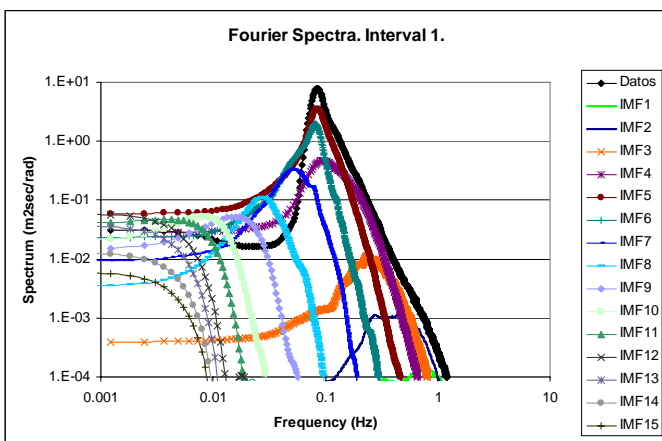


Fig. 9 Fourier Spectrum for the original data and IMFs, Interval 1.

It can be seen that the energy order coincides with that given before and also that IMFs 4, 5 and 6 have a peak frequency similar to that of the

whole data set. In table 5 we give some spectral characteristics (significant wave height, mean wave period and peak period) for the original data and all IMFs.

Table 5 Significant wave height, mean wave period and peak period for the original data and all IMFs, Interval 1.

	Hs	T01	Tp
Data	5.34	9.31	11.69
IMF1	0.11	1.15	1.31
IMF2	0.24	1.98	2.32
IMF3	0.50	3.34	3.92
IMF4	2.24	7.52	9.63
IMF5	3.87	10.65	11.60
IMF6	2.62	12.82	12.54
IMF7	1.19	17.65	18.96
IMF8	0.51	32.41	35.35
IMF9	0.33	61.11	63.67
IMF10	0.25	107.25	157.60
IMF11	0.21	146.52	278.29
IMF12	0.17	180.70	354.70
IMF13	0.13	186.02	364.85
IMF14	0.07	188.47	367.93
IMF15	0.05	188.61	368.95
IMF16	0.05	189.53	369.30
IMF17	0.04	189.82	369.38

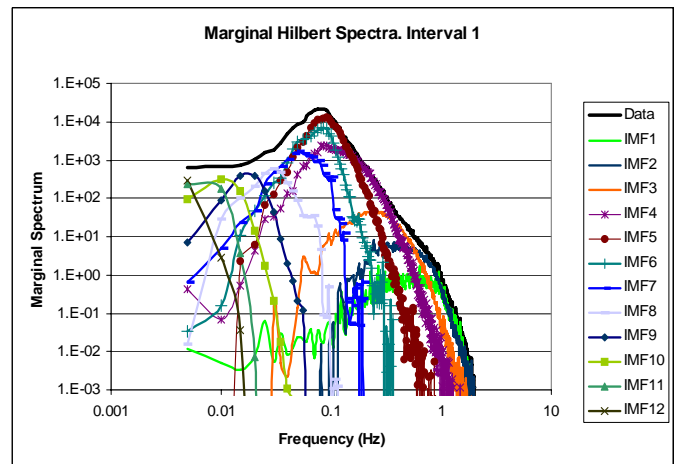


Fig. 10 Marginal Hilbert Spectrum for the original data and all IMFs, Interval 1.

Figure 10 gives the marginal Hilbert spectra for the data and the first 12 IMFs. These spectra are projections of the time-frequency energy distribution given in Figure 8, and should be interpreted differently. If there is energy associated to a given frequency in the Fourier spectrum, then there is a trigonometric component with this frequency and amplitude for the complete time span of the data. In the case of the marginal Hilbert spectrum, energy at a given frequency means that in the time span of the data there is a probability proportional to the amount of energy of having a component with this frequency and amplitude at any time.

The IMFs represent different oscillatory modes present in the original data and have different energy. This can be seen from both the Fourier and the marginal Hilbert spectra. The first Intrinsic Mode Functions cover the tail of the data spectrum while IMFs 4, 5 and 6 are located at the central part of the spectrum, with similar peak frequency. IMF 7 also makes an important contribution to the central part of the spectrum, but with a lower frequency range. Higher IMFs correspond to lower frequencies, also with lower energy.

CONCLUSIONS

We have considered a set of data coming from a storm in the North Sea in 1999. These data were analyzed using the Hilbert Huang Transform, a method developed for the analysis of nonlinear and non-stationary time series.

Each of the five data intervals was decomposed into IMFs and their contribution to the total energy was assessed. The order in this energy contribution reflect the characteristics of the particular data set been considered. Other spectral characteristics were also considered.

The number of Intrinsic Mode Functions needed to decompose a given data set seems to be related to its size and is larger than what has been reported for normal sea states by other authors. The energy distribution among different IMFs is also different than what has been reported so far. This may be due to the fact the sea states produced during a storm are more complex, hence need more IMFs to be decomposed and their energy distribution is different than that for normal sea states. Further investigation is needed with other data sets to confirm this.

ACKNOWLEDGEMENTS

The authors would like to thank Total E&P UK for the wave data from the Alwyn North platform.

The Hilbert-Huang Transform - Data Processing System is copyright United States Government as represented by the Administrator of the National Aeronautics and Space Administration and was used with permission.

The software WAFO developed by the Wafo group at Lund University of Technology, Sweden was used for the calculation of all Fourier

spectra and associated spectral characteristics. This software is available at <http://www.maths.lth.se/matstat/wafo>.

This work was partially supported by CONACYT Mexico, grant 52554.

REFERENCES

- Huang, NE, Shen Z, Long SR, Wu MC, Shin HS, Zheng Q, Yuen Y, Tung CC, Liu HH (1998). "The empirical mode decomposition and Hilbert spectrum for nonlinear and non-stationary time series analysis," *Proc R Soc Lond*, Vol. 454, pp 903-95.
- Huang, NE, Shen Z, Long SR (1999). "A new view of nonlinear water waves: the Hilbert spectrum," *Ann Rev Fluid Mech* Vol. 31, pp 417-57.
- Huang, NE, Wu ML, Long SR, Shen SP, Per WQ, Gloersen P, Fan KL (2003). "A confidence limit for the empirical mode decomposition and Hilbert spectral analysis," *Proc R Soc Lond* Vol. 459 pp 2317-45.
- Huang, NE (2005a) "Introduction to Hilbert-Huang Transform and some recent developments," In: Huang N., Attoh-Okine N.O., editors. *The Hilbert-Huang transform in Engineering*. CRC Press, pp 1-23.
- Huang, NE (2005b) "Introduction to Hilbert-Huang Transform and its related mathematical problems," In: Huang NE, Shen SSP, editors. *Hilbert-Huang Transform and Its Applications*. World Scientific, pp 1-26.
- Schlurmann, T (2000). "The empirical mode decomposition and the Hilbert spectra to analyse embedded characteristic oscillations of extreme waves," In: *Rogue Waves*, Edition Inframer, ISBN: 2-84433-063-0, pp. 157-165.
- Veltcheva, AD & Guedes Soares, C (2004). "Identification of the components of wave spectra by the Hilbert Huang transform method," *Applied Ocean Res*. Vol. 26 pp 1-12.
- Veltcheva, AD (2005) "An application of HHT method to the nearshore sea waves," In: Huang N., Attoh-Okine N.O., editors. *The Hilbert-Huang transform in Engineering*. CRC Press, pp 97-119.
- Wolfram, J, Feld, G and Allen, J (1994). "A new approach to estimating environmental loading using joint probabilities," *7th Int. Conf. on Behaviour of Offshore Structures*, Pergamon, Boston, Vol. 2. pp. 701-713.